

An Active Safety System Using Two Laser Scanners for a Robot Tractor

Liangliang YANG, Noboru NOGUCHI*

Vehicle Robotics Laboratory, Graduate School of Agriculture, Hokkaido University, Kita-9, Nishi-9, Kita-ku, Sapporo, 060-8589, Japan; (e-mail: yang@bpe.agr.hokudai.ac.jp, noguchi@bpe.agr.hokudai.ac.jp)

Abstract: A 2D laser scanner was used for obstacle detection for autonomous vehicles for its high accuracy at both indoor and outdoor environment on the measurement of distance. Traditionally, the obstacle detection method was depended on the distance from an object to a laser scanner, and an obstacle was defined if the measured distance was less than a threshold. A shortage of the traditional obstacle detection method for a robot tractor is that a low obstacle cannot be detected when the height of the obstacle is lower than the height of the scanning plane of the 2D laser scanner. In this article, obstacle detection method using two 2D laser scanners is discussed. One laser scanner is mounted at the front and the other is mounted at the rear of the vehicle in order to cover the whole surroundings of the vehicle. The laser scanner was mounted look-at-down in order to detect a low obstacle. A test was carried out at an outdoor environment to verify the developed safety system. The test results indicate the developed system could detect obstacles with accuracy around 10 cm.

1. INTRODUCTION

Development of a robot tractor is a practical way to solve the problem of decreasing number of human labourers for agriculture and to reduce the fatigue of farmers. The safety is a decisive factor for utilizing a robot tractor in a real farm. Researchers have utilized some kinds of sensors for providing a safety system for a tractor, such as, a laser (Kise et al., 2005), cameras (Yang and Noguchi, 2012), a laser scanner fusion with a camera (Maria et al., 2011) and GPSs for a master-slave robots (Noguchi et al., 2004). The laser scanner can provide a real-time accurate measurement. And, it is an active and all-day usable sensor. Therefore, it is suitable to be used as an obstacle detection sensor. A traditional method for using the laser scanner is that the laser scanner is mounted at the front of a vehicle and its scanning plane is set parallel to the ground where the vehicle is running. It is an easier way to develop obstacle detection algorithms for obstacle detection under this mounting method. However, a shortage of the traditional method is that an obstacle will not be detected when it's lower than the scanning plane. In this study, two laser scanners were mounted at the front and back of a robot tractor in order to cover the surrounding of the vehicle. In addition, both laser scanners were set look-at-down (LAT) in order to detect a low obstacle. However, the LAT mounting method arise a problem that the surface of the ground may be detected as an obstacle. In order to solve this problem, an obstacle detection algorithm using wavelet transform was proposed in this study.

2. EXPERIMENT PLATFORM AND SENSORS

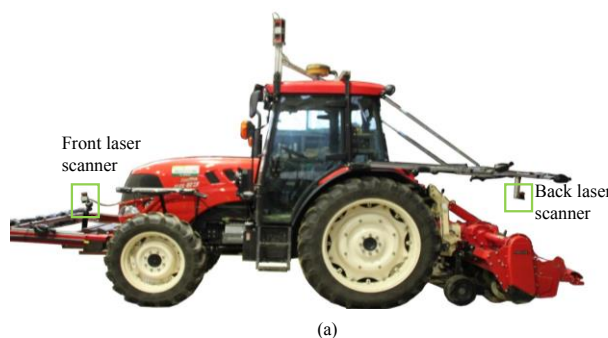
Two 2D laser scanners (UTM-30LX, Hokuyo automatic Co., Ltd., Japan) were utilized in this research to detect obstacles in surrounding of a robot tractor as shown in Fig. 1. The robot tractor was developed based on a commercial 61 kW wheel type tractor (EG83, Yanmar Co., Ltd., Japan).

Two laser scanners were mounted along the symmetry axis of longitudinal direction at the front (Fig. 1b) and back (Fig. 1c), respectively. In order to detect a low obstacle above the surface of ground, the scanning plane of front and back laser scanners were rotated 5~15 degree (infield adjustable) along anti-clockwise and clockwise direction from the ground plane as shown in Fig. 1d and Fig. 1e, respectively.

The specification of the laser scanner that was used in this study is shown in Fig. 2. The detection angle is 270°, angular resolution is 0.25°, and the max guaranteed distance is 30 m. The coordinates of the laser scanner is defined in polar coordinate system. The front of the scanner is defined as 0°, turning along anti-clockwise is + and turning along clockwise is -.

The coordinate of point P was transformed from laser coordinates (polar coordinates) to Cartesian coordinates by Eq. (1):

$$\begin{cases} x = \rho \times \cos(\theta) \\ y = \rho \times \sin(\theta) \end{cases} \quad (1)$$



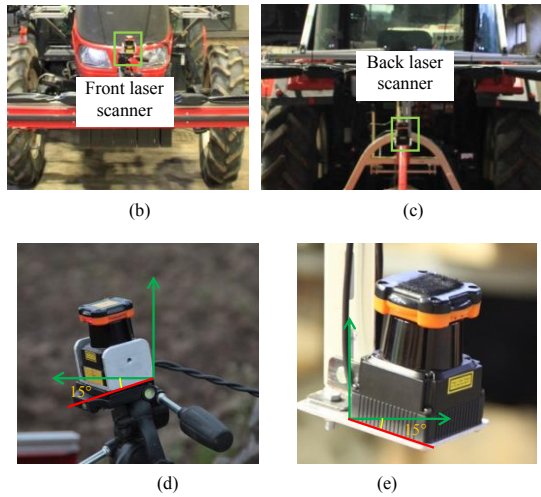


Fig. 1 Two 2D laser scanners mounted on a robot tractor. (a) Left side view; (b) Front view; (c) Back view; (d) Front laser scanner; (e) Back laser scanner.

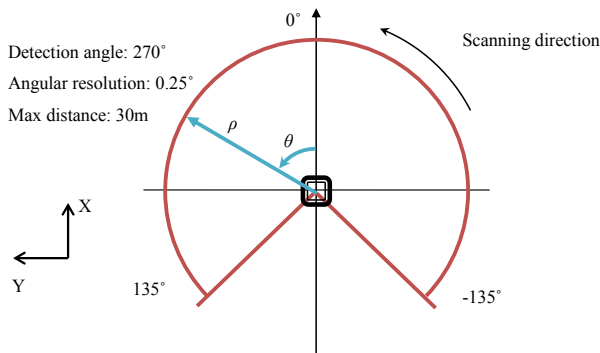


Fig. 2 The specification of the 2D laser scanner.

3. OBSTACLE DETECTION METHODS

The obstacle detection methods were described as:

At first, the raw laser data was firstly grabbed from two laser scanners.

At second, the raw data of each laser scanner was transformed to Cartesian coordinates and segmented to five areas as shown in Fig. 3, named left, centre, right, front and rear areas.

At third, the wavelet transform (WT) was utilized to detect an obstacle in the front and rear areas.

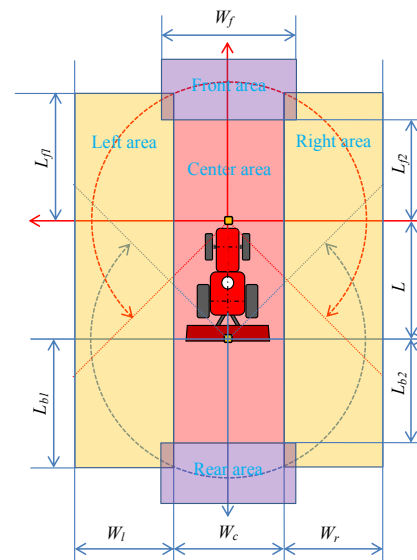
At fourth, the other obstacle detection method was applied at left, centre and right areas, which was named as range-based obstacle detection (ROD) method in this study.

Finally, the detection results were sent to the robot tractor via a CANBUS to control the tractor according to the safety condition. The safety condition was defined by a safety index as shown in Table 1.

Table 1. Definition of Safety index.

Safety index	0	1	2	3
Safety condition	Not available	Safe	Warning	Danger
Vehicle speed (m/s)	0	According to setting (normal)	0.3	0
Obstacle position	Not available	Outside of the five areas	Left or right area	Center area or detected by WT at front or rear area

As shown in Table 1, there were four levels of safety conditions. The safety index '0' means that the safety system has troubles. And in this condition the vehicle should be stopped. The safety index '1' means that there is not obstacle inside of the defined areas; in this condition the vehicle speed will be adjusted according to the working, such as seeding, rotary tillage, etc. The safety index '2' indicates that an obstacle is detected at the area of left or right area; the vehicle speed will be set to a lower speed, such as 0.3 m/s, so that the robot tractor can be stopped as fast as possible if the obstacle moves too close to the tractor. And the lower speed can be adjusted according to the real condition. The safety index is denoted as '3' if an obstacle appears at the centre area or is detected at front or rear area by the WT method.



In this study: $W_f=3.5m$, $L_{l1}=6m$, $L_{l2}=5m$, $L_{b1}=6m$, $L_{b2}=5m$, $L=5.5m$, $W_i=2m$, $W_c=3m$, $W_r=2m$.

Fig. 3 Segmentation of detection area of laser scanners.

3.1 Range-based obstacle detection method

Let's denote one scanning data as a data set Ω :

$$\Omega = \{\omega_i | \omega_i = (\rho_i, \theta_i), \quad i = 0, 1, \dots, n\} \quad (2)$$

$$\theta_i = f(i) = (i-1)/4 - 135. \quad (3)$$

where, ω_i is the scanning data element; ρ_i and θ_i are the range and the angle of point i in the coordinates of the laser scanner; i is the index of scanning points; n is the maximum points number which is 1081 in this study.

And, a subset of Ω, Ω' , denotes a collection of subset A_t which refers to an obstacle:

$$\Omega' = \bigcup_{t \in T} A_t. \quad (4)$$

where, T is an index set that represents the total number of obstacles; t is an index of an obstacle.

$$A_t = \{\omega_j \mid \omega_j = (\rho_j, \theta_j), \quad j = m, m+1, \dots, m+l-1\}, \quad t \in T \quad (5)$$

where, m is the start point index of obstacle- t , l is the length of total points of the obstacle- t .

As shown in Fig. 4, two threshold t_1 and t_2 , which are set to according to the detection area setting, segment the raw data set Ω to three subsets, Ω_1, Ω_2 and Ω_3 ,

$$\Omega = \Omega_1 \cup \Omega_2 \cup \Omega_3, \quad (6)$$

$$\Omega_1 = \{\omega_j \mid (\rho_j, \theta_j)\}, \quad (\rho_j < t_1 \quad \text{AND} \quad \rho_j > 100, j \in N)$$

$$\Omega_2 = \{\omega_j \mid (\rho_j, \theta_j)\}, \quad (\rho_j \geq t_1 \quad \text{AND} \quad \rho_j \leq t_2, j \in N)$$

$$\Omega_3 = \{\omega_j \mid (\rho_j, \theta_j)\}, \quad (\rho_j > t_2, j \in N)$$

where, N is the index set, t_1 and t_2 are set as 5000 and 11000, respectively in this study.

Ω_1 will be processed by using ROD method that will be introduced at the next section. Ω_2 is the data set that will be processed by WT method. Ω_3 will not be processed because the point is far to the laser scanner.

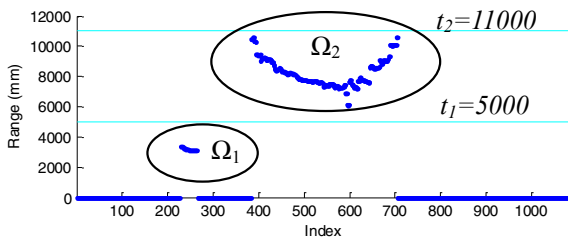


Fig. 4 Segmentation of a raw data set of one scanning.

The range based obstacle detection (ROD) method segmented an obstacle from the point data set based on the first difference of range ρ as shown in Fig. 5. The first difference is defined as Eq.(7):

$$\Delta\rho_i = \rho_{i+1} - \rho_i. \quad (7)$$

Fig. 5a illustrates the data set of Fig. 4 in Cartesian coordinates. Fig. 5b shows a segmented obstacle and the corresponding first difference of Fig. 5a. The start and end index of the obstacle is determined by a data set D :

$$D = \{d_j \mid d_j = (\Delta\rho_i, i)\}, \quad i \in N, \quad j \in N$$

$$\Delta\rho_i > t_{d2} \text{ (if } \Delta\rho_i > 0)$$

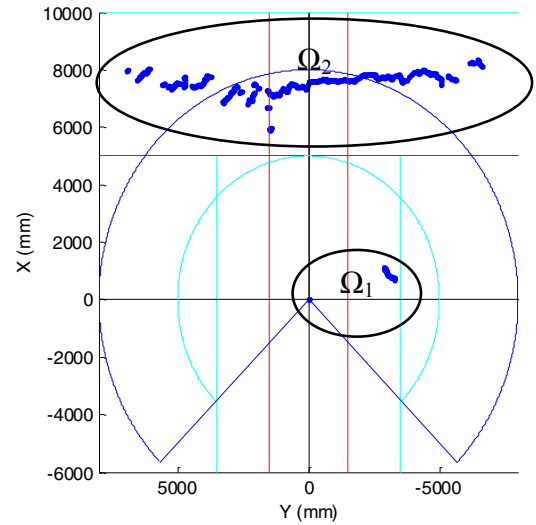
$$\text{OR } \Delta\rho_i < t_{d1} \text{ (if } \Delta\rho_i < 0) \quad (8)$$

where, i is the index of $\Delta\rho$, t_{d1} and t_{d2} are set as 1000 and -1000 mm in this study respectively.

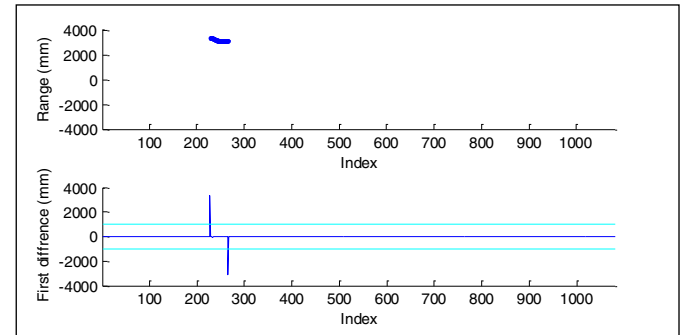
The start index (j_s) is the odd index value, and the end index (j_t) is the the even index value of element i in D . Such as, the start and end index are 229 and 266, respectively, in Fig. 5b. This obstacle is denoted as,

$$A_t = \{\omega_n \mid \omega_n = (\rho_n, \theta_n)\}, \quad n \in [j_s, j_t] \quad (9)$$

where, t is the obstacle number, that is 1 in this example.



(a)



(b)

Fig. 5. Segmentation an obstacle from the raw point data set. (a) the data set in Cartesian coordinates; (b) segmented obstacle and its first difference.

The declared distance (ρ_d) from obstacle to laser scanner is calculated by the mean value of the segmented obstacle data set, angle (θ_d) is calculated from the middle value of j_s and j_t by Eq. (3). The safety index (S) of the obstacle is calculated by Eq. (10) for the front laser scanner:

$$S = f(x, y) = \begin{cases} 1, & |y| > w_l + 1/2 \times w_c, \quad (x, any) \\ 2, & w_l + 1/2 \times w_c \geq |y| > 1/2 \times w_c, \quad (x < l_{f1}) \\ 3, & |y| \leq 1/2 \times w_c, \quad (x < l_{f2}) \end{cases} \quad (10)$$

x and y are calculated by Eq. (1) using ρ_d and θ_d . l_{f1} and l_{f2} will be l_{b1} and l_{b2} for the back laser scanner.

3.2 Obstacle detection method using wavelet transform

Wavelet analysis is an exciting method for solving difficult problems in mathematics, physics, and engineering. The concept of ‘wavelet’ was introduced by Jean Morlet in 1982 (Daubechies, 1992). The continuous wavelet transform (CWT) is provided by Eq. (11):

$$WT_x(a, \tau) = \frac{1}{\sqrt{a}} \int_{-\infty}^{+\infty} x(t) \psi^* \left(\frac{t-\tau}{a} \right) dt, \quad a > 0 \quad (11)$$

where, $x(t)$ is the signal to be analysed. $\psi(t)$ is the mother wavelet. All the wavelet functions applied in the transformation are derived from the mother wavelet through translation (shifting) τ , and scaling (dilation or compression) a . * represents operation of complex conjugate.

In numerical analysis, a discrete wavelet transform (DWT) is any wavelet transform for which the wavelets are discretely sampled. A wavelet, in the sense of the DWT, is an orthogonal function which can be applied to a finite group of data (Edwards, 1991). It is like the Discrete Fourier Transform (DFT), in that the transforming function is orthogonal. Whereas the basis function of the Fourier Transform is a sinusoid, the wavelet basis is a set of functions which are defined by a recursive difference equation, which is written as Eq.(12):

$$\phi(x) = \sum_{k=0}^{M-1} c_k \phi(2x-k) \quad (12)$$

where, M is the range of the summation, c is the wavelet basis, ϕ is the input signal. The coefficients of Daubechies-4

wavelet that used in this study are $\frac{1}{4}(1+\sqrt{3})$, $\frac{1}{4}(3+\sqrt{3})$, $\frac{1}{4}(3-\sqrt{3})$ and $\frac{1}{4}(1-\sqrt{3})$, respectively.

The Mallat ‘pyramid’ algorithm (Mallat, 1989) is a computationally efficient method of implementing the wavelet transform. The pyramid algorithm operates on a finite set of N input data, where N is a power of two; this value will be referred to as the input data size. These data are passed through two convolution functions, each of which creates an output stream that is half the length of the original input data. These convolution functions are filters; one half of the output is produced by the ‘low-pass’ filter function written as Eq.(13):

$$a_i = \frac{1}{2} \sum_{j=1}^N c_{2i-j+1} f_j, \quad i = 1, \dots, N/2 \quad (13)$$

and the other half is produced by the ‘high-pass’ filter function, related to Eq.(14):

$$b_i = \frac{1}{2} \sum_{j=1}^N (-1)^{j+1} c_{j+2-2i} f_j, \quad i = 1, \dots, N/2 \quad (14)$$

where N is the input data size, c is the coefficients of wavelet function, f is the input signal, and a and b are the output signal.

In this study, Ω_2 of Eq. (6) will be processed by using WT to detect obstacles in the front and rear areas. A data pre-process step was performed to limit the width of Ω_2 by limit the width using Eq. (15). Fig. 6 shows a segmented area (red points in the figure) which will be processed for obstacle detection using WT.

$$\begin{aligned} \Omega_2' &\subset \Omega_2 \\ \Omega_2' &= \{\omega_i | \omega_i = (x_i, y_i)\}, \quad t \in T', \\ y_i &< 1/2 \times W_f, (y_i \geq 0) \\ y_i &> -1/2 \times W_f, (y_i < 0) \end{aligned} \quad (15)$$

where x_i and y_i are calculated by Eq. (1) from and ρ_t and θ_i ; W_f is shown in Fig. 3; T' is a subset of index set T .

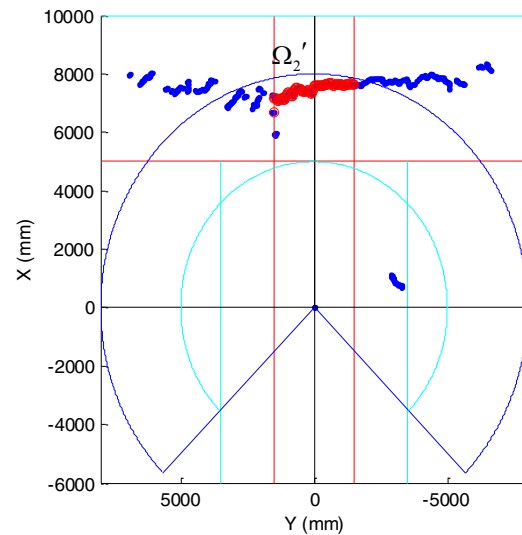


Fig. 6 Pre-processed data for detection using WT (Red points).

The WT results are shown in Fig. 7. The ‘original signal’ shows the data Ω_2' shown in i - R coordinates of which the horizontal-axis is the index of Ω_2' ; the vertical-axis is the range. ‘cA1’ is the approximation coefficients of the first level WT, while ‘cD1’ is the detail coefficients of the first level WT. ‘cA2’ and ‘cD2’ are the approximation coefficients and detail coefficients the second level WT.

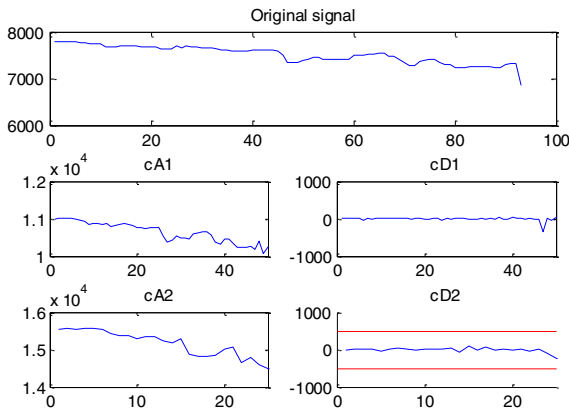


Fig. 7 WT results of the data set Ω_2' .

For comparing, a scanning data when an obstacle is at front of the laser scanner is shown in Fig. 8. Fig. 9 depicts the WT results of this data. From the second level of detail coefficients, cD2, in Fig. 7 and Fig. 9, it can be seen that cD2 is near to 0 when there is no obstacle. In contrast, the cD2 has pulse values at the place where has an obstacle. In this way, the cD2 was adopted in this study for obstacle detection. A threshold, 500, was set to detect the pulse value.

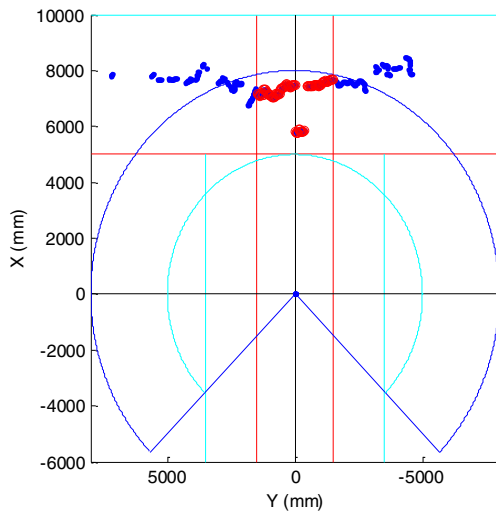


Fig. 8 A scanning data when an obstacle is at the front area.

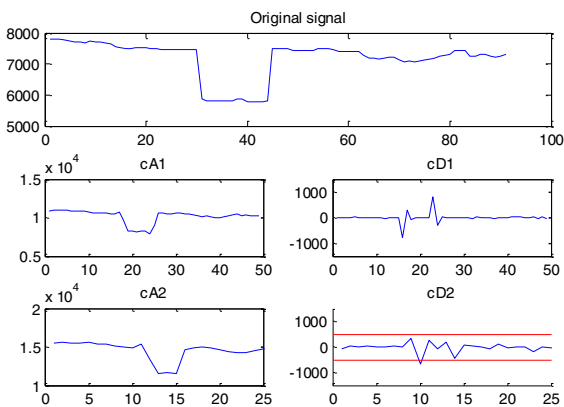


Fig. 9 WT results of the segmented front data set of Fig. 8.

4. EXPERIMENT RESULTS AND DISCUSSION

An outdoor test was conducted at daytime of a low grass covered field of Hokkaido University (Sapporo, Japan) to show the working function of the developed safety system. The test condition is shown in Fig. 10a. A young man who wore a helmet was an obstacle in the test. And a GPS antenna was mounted at the top of the helmet (Fig. 10b) in order to measure the position of the obstacle. The position of the human was measured by a RTK-GPS (Legacy, Inc., Japan) with an accuracy of ± 0.03 m. The position data of the human was transmitted to the PC for obstacle detection by a Bluetooth transmitter at speed of 115,200 bps. The obstacle was working in the safe, warning and stop region in the test, respectively.

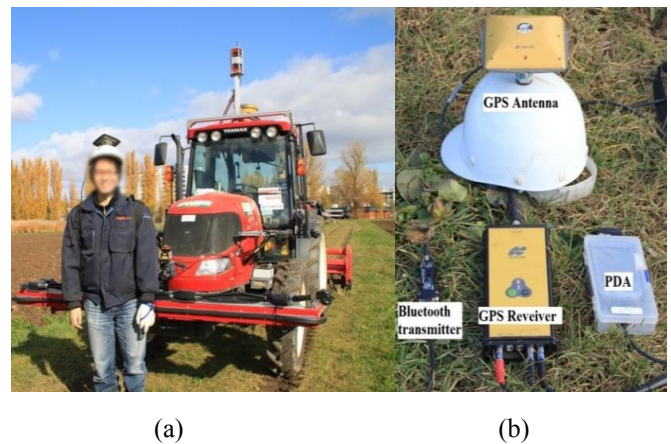


Fig. 10 Obstacle detection test system. (a) A human (obstacle) and robot tractor; (b) A RTK-GPS for measuring the position of the human.

The trajectories of the tractor and human were shown in Fig. 11. And the tractor speed and safety index were shown in Fig. 12, when a zoom-in area that shows the speed down area. It can be seen from Fig. 12 that the tractor can be controlled correctly in logic according to the safety index. The safety index is changed from 1 to 3 at 19.9 s, and at about 20.3 s the vehicle speed starts decreasing from the normal speed (1 m/s) to about 0 m/s at 21.6 s. It cost about 0.4 s from the safety index changed to 3 (19.9 s) to the vehicle started to stopping (20.3 s). This is the time cost by the data transmission and mechanical delay of the vehicle. The slowdown procedure continued about 1.3 s from 20.3 s to 21.6 s. The tractor ran about 1.05 m from obstacle was been detected to tractor stopped when the vehicle speed was 1 m/s. The stop distance was acceptable for a robot tractor.

In order to compare the distance measured from the laser scanner, firstly the distance from the human to the laser scanner was measured by the RTK-GPSs. In addition, the distance measured by the laser scanner and the distance error between these two distances are also shown in this Fig. 14.

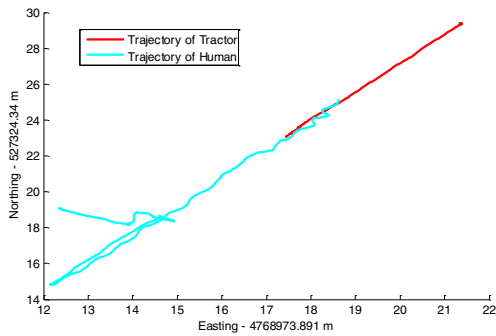


Fig. 11 Trajectory of the tractor and human.

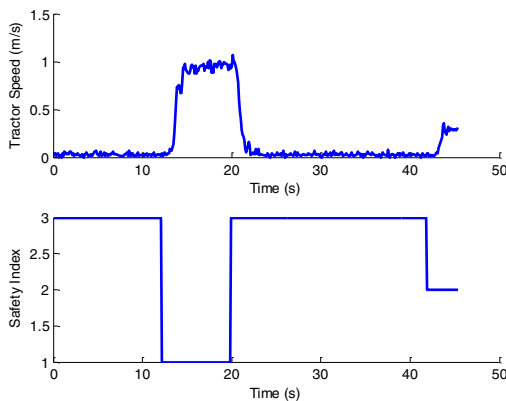


Fig. 12 Tractor speed and safety index of the test.

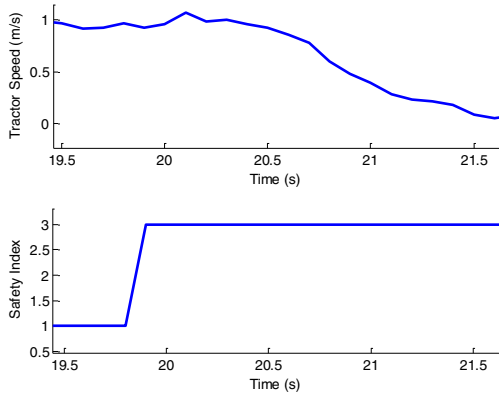


Fig. 13 Zoom-in of the speed down area of Fig. 12.

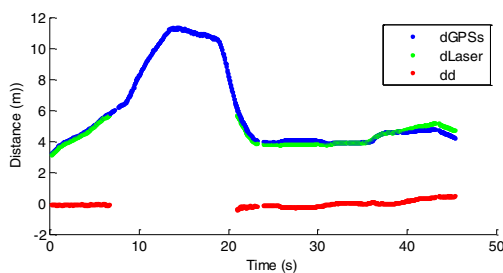


Fig. 14 Distance from the front laser scanner to the human by RTK-GPSs, laser scanner and their difference.

In Fig. 14, 'dGPSs', 'dLaser' and 'dd' refer to the distance measured by the RTK-GPSs, the laser scanner and their difference respectively. There is a gap in Fig. 14 of 'dLaser' and 'dd' because obstacle was not in the ROD area. Fig. 15 shows the distance error, from which it can be seen that the error is around -0.1 m. The error increased a little after 40 s in Fig. 14, but it is still less than 0.5 m. This is enough for detection obstacle for a robot tractor.

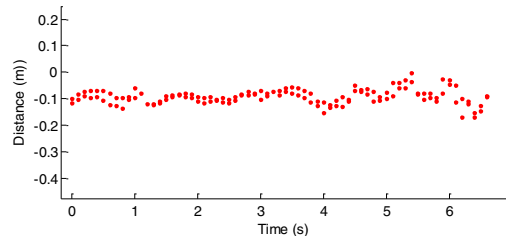


Fig. 15 Distance error.

6. CONCLUSIONS

In this study, two laser scanners were adopted to develop an obstacle detection system for a robot tractor. A range-based obstacle detection (ROD) and a wavelet transform (WT) based obstacle detection method were developed. And a test employed to show the working function of the developed obstacle detection method was conducted at daytime at a flat low grass covered field when the tractor speed was 1 m/s. The test results show that the distance error of obstacle was about 0.1 m. The speed down and stop decision could be made correctly in the test.

REFERENCES

- Daubechies, I., 1992. *Ten Lectures on Wavelets*. SIAM.
- Mallat, S.G., 1989. A theory for multiresolution signal decomposition: the wavelet representation. *Pattern Analysis and Machine Intelligence, IEEE Transactions* 11, 674-693.
- Maria C. Garcia-Alegre, David Martin, D. Miguel Guinea and Domingo Guinea (2011). *Real-Time Fusion of Visual Images and Laser Data Images for Safe Navigation in Outdoor Environments, Sensor Fusion-Foundation and Applications*, Dr. Ciza Thomas (Ed.), ISBN: 978-953-307-446-7.
- Kise, M., Zhang, Q., Noguchi, N., 2005. An obstacle identification algorithm for a laser range finder-based obstacle detector. *Transactions of the Asae* 48, 1269-1278.
- Noguchi, N., Will, J., Reid, J., Zhang, Q., 2004. Development of a master-slave robot system for farm operations. *Computers and Electronics in Agriculture* 44, 1-19.
- Yang, L., Noguchi, N., 2012. Human detection for a robot tractor using omni-directional stereo vision. *Computers and Electronics in Agriculture* 89, 116-125.